ELSEVIER

The Development of Atom Probe Field-Ion Microscopy

M. K. Miller
Microscopy and Microanalytical Sciences Group, Metals and Ceramics Division, Oak Ridge National Laboratory, Oak Ridge, TN 37831-6376

A review of the development of the techniques of atom probe field-ion microscopy and atom probe tomography is presented. The development is traced from the original time-of-flight atom probe field-ion microscope developed by Müller, Panitz, and McLean in 1968 to the energy-compensated three-dimensional atom probes that are commercially available today. The various types of atom probes that have been developed are described. Published by Elsevier Science Inc.

INTRODUCTION

Atom probe field-ion microscopy and atom probe tomography[1] have developed into a pair of the most powerful microanalytical techniques available for the characterization of materials. These two techniques refer to the original technique and the recently introduced three-dimensional (3D) variants. The state-of-the-art 3D atom probes enable the position and the identity of millions of atoms obtained from a sample of the material to be reconstructed and analyzed with near atomic precision. The ability to determine the precise location of all the solutes in a material is one of the critical steps in designing new and improved alloys.

Atom probe techniques have been applied to many diverse metallurgical problems [1–3]. These techniques are mainly applied to materials in which the solutes are not uniformly distributed, and where high resolution information about the solute distribution is required. Typical applications are the investigation of the early stages of precipitation or phase separation, solute partitioning between phases, segregation to grain boundaries or interphase interfaces, clustering, and ordering. Several reviews of the applications of the atom probe technique may also be found elsewhere in this volume. In addition to these primarily metallurgically oriented studies, these techniques have been applied to surface chemistry [4, 5].

In this paper, the historical development of the atom probe techniques from the inception in 1968 to the new generation of 3D atom probes is reviewed. Some illustrative examples of the types of analyses that may be performed with these techniques are also presented. Although there are many atom probe laboratories around the world in universities, national laboratories, and industrial corporations, the technique is not as widely available as transmission electron microscopy (TEM). However, the number of atom probes is approximately comparable to the number of the more specialized high-resolution analytical electron microscopes.

DEVELOPMENT OF THE ATOM PROBE

The atom probe traces its origins back to the original field ion microscope (FIM) in-

[1]Tomography: a method of producing three-dimensional images of the internal structures of a solid object.

MATERIALS CHARACTERIZATION 44:11–27 (2000)
Published by Elsevier Science Inc.
655 Avenue of the Americas, New York, NY 10010
1044-5803/00/$–see front matter
PII S1044-5803(99)00053-4

vented in 1951 by Prof. Erwin W. Müller at Pennsylvania State University [6], and before that to the field electron emission microscope (FEM) invented in 1936 by Müller in Berlin [7]. In 1955, Bahadur and Müller obtained the first images of individual tungsten atoms in a field ion microscope. In addition to the atom probe, many other instruments such as the scanning tunneling microscope and its derivatives, and the liquid metal and gaseous ion sources have been derived from Müller's initial concepts.

Because the field ion microscope is an integral part of an atom probe, a brief description of its operation is required. The basic configuration of a field ion microscope is a needle-shaped specimen positioned approximately 50mm from a phosphor screen in an ultrahigh vacuum system. Since 1969, microchannel plate image intensifiers have been used as detectors, and are placed immediately in front of the phosphor screen to increase the gain of the image by a factor of $\sim$1000. The specimen is connected to both a cryostat and a high-voltage supply. After evacuating the vacuum system to a base pressure below 10^{-7}Pa and cooling the specimen to a temperature in the range 10 to 20K for aluminum alloys and 40 to 60K for most other alloys, a trace ($\sim 2 \times 10^{-3}$Pa) of image gas is admitted into the system. Both the temperature and base pressure are extremely important parameters in obtaining reliable information from this technique. The choice of the image gas depends on the material being analyzed, and is usually helium for the refractory metals and neon for most other systems. The voltage applied to the specimen is increased until an image appears on the phosphor screen. Due to the enhancement of the field in the vicinity of the apex of the needle-shaped specimen, the image gas atoms are polarized and attracted to the specimen where they become thermally accommodated to the cryogenic temperature. If the field is high enough ($\sim$37Vnm^{-1} for neon), the image gas atoms on the surface of the specimen can be field ionized by an electron tunneling process. As soon as they become positively charged, the ions are repelled away from the positively charged specimen towards the phosphor screen. Upon impacting the phosphor screen they produce a spot of light. This process occurs across the entire surface of the needle, and the resulting pattern on the phosphor screen is the field ion image.

Some examples of field ion micrographs are shown in Fig. 1. Most field ion micrographs of crystalline materials exhibit characteristic rings where atomic planes intersect the surface of the needle, as shown in a field ion micrograph of iridium in Fig. 1(a). Because these atom locations protrude slightly more from the mean surface of the needle, the field ionization process occurs preferentially at these locations. These rings are not evident in amorphous materials, as shown in the field ion micrograph of a bulk metallic glass in Fig. 1(b). Grain boundaries are detected by the abrupt discontinuities in these rings due to the change in orientation of the crystal structure of the two grains, as shown in Fig. 1(c). The orientation relationship between the grains may be determined from the positions of the crystallographic poles (i.e., the centers of the rings) in the two grains. Segregation may also be detected by the presence of bright spots decorating the line of the boundary. In phase-separated material, the different phases generally exhibit different contrast, as shown for the 5nm-diameter secondary precipitates and the matrix in the nickel-based superalloy in Fig. 1(d). The contrast arises, as the different phases generally require slightly different fields to field evaporate and, therefore, protrude slightly more or less from the mean surface. Consequently, the field is higher over the protruding regions and, therefore, more image gas is ionized and these regions appear bright in the field ion image. The size and shape of the precipitates or other features may be determined by field evaporating the surface and tracing the outline of the precipitate in the sequence of field ion images after known amounts of material have been field evaporated. Because the field evaporation process can be precisely controlled,

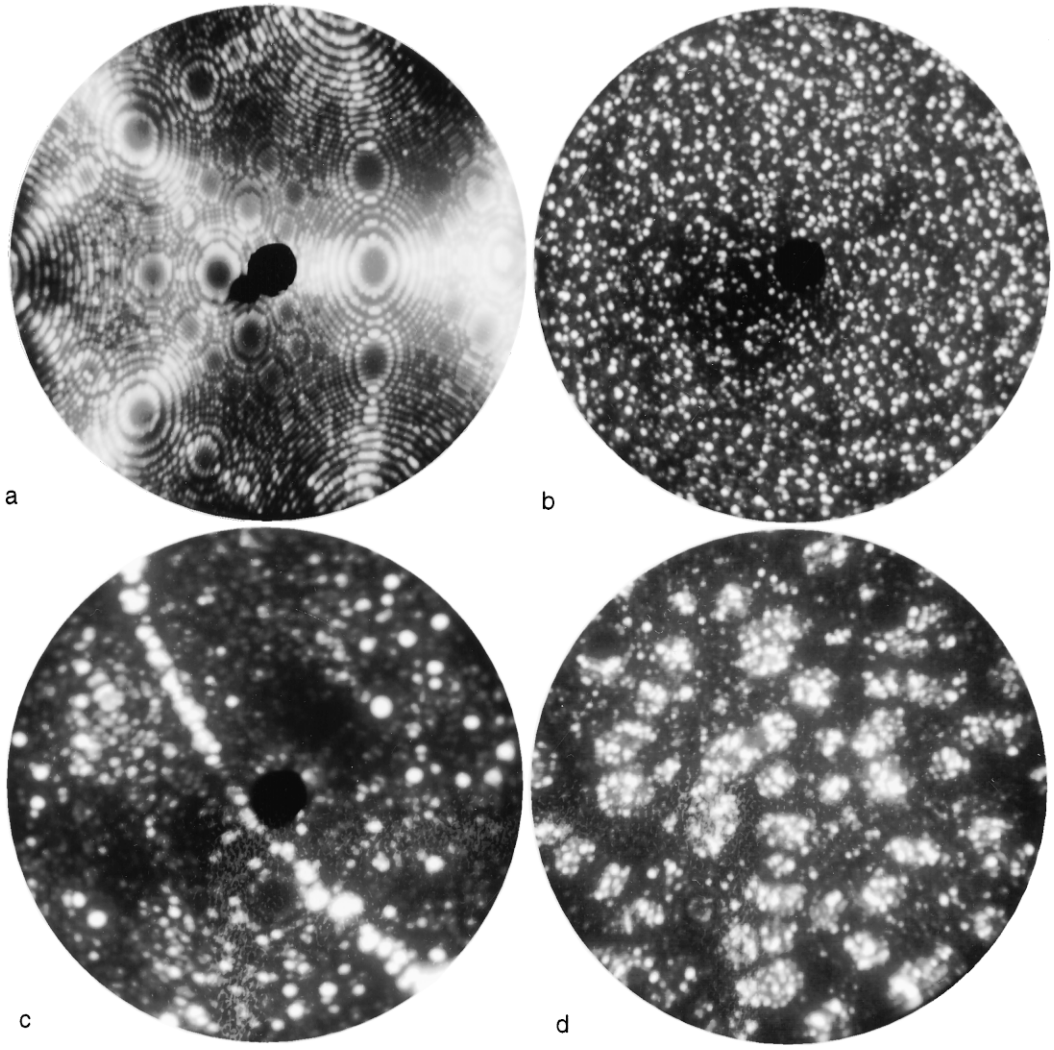

FIG. 1. Examples of field ion micrographs of (a) iridium, (b) a $Pd_{40}Ni_{40}P_{20}$ bulk metallic glass, (c) a decorated grain boundary in a neutron-irradiated pressure vessel steel, and (d) 5nm-diameter secondary precipitates in the nickel-based superalloy Alloy 718

the amount of material removed between these images can be accurately determined by counting the number of rings that were removed, assuming the interplanar spacing of that crystal plane is known.

The magnification of this projection microscope, M, is given by the ratio of the specimen to screen distance, R, and the end radius of the specimen, r, that is, $M = R/\beta r$, where β is an image compression factor that is usually in the range 1.5 to 2. Therefore, a typical field ion specimen with an end radius of 33nm would produce a magnification of $\sim 1 \times 10^6$. If the field is raised further, the surface atoms from the specimen may also be field ionized and removed. As material is field evaporated from the specimen, the end radius invariably increases so that the applied voltage has to be increased, and there is a corresponding reduction in the magnification (unless the phosphor screen is moved further from the specimen to compensate).

Field evaporation may be used to smooth out any irregularities introduced during specimen preparation, and also to reveal

microstructural features in the interior of the specimen. Field evaporation is also the process that is used in the atom probe to remove atoms for analysis in the mass spectrometer.

ORIGINAL ATOM PROBE

Müller, Panitz, and McLean developed the first atom probe in 1968 [8, 9]. It should be noted that mass spectrometry of the species produced by field ionization had been performed previously by Müller in 1960 [10] and by Vanselow and Schmidt in 1966 [11]. More significantly, Barofsky and Müller also combined a magnetic sector mass spectrometer with a field ion microscope in 1968 to determine the nature of these species at low temperatures [12]. However, these instruments are not normally considered to be true atom probes, as they did not have the ability to select individual atoms or regions of the specimen.

The Müller, Panitz, and McLean instrument featured a field ion microscope with a time-of-flight mass spectrometer, as shown in Fig. 2. The mass spectrometer was a field-free drift tube terminated with a single atom detector. This microscope permitted the identities of selectable individual atoms to be determined for the first time. The field ion specimen is mounted on a goniometer so that all positions on the specimen's surface may be aligned with the small entrance aperture to the mass spectrometer. Although the physical size of this circular aperture is typically 1 to 2mm, its effective size on the specimen is reduced by the magnification of the field ion microscope (i.e., 1 to 4nm in diameter). Vibration of the specimen is not a problem in the atom probe, as the imaging process does not amplify its magnitude. This atom probe has several unique features compared to subsequent instruments. It is the only atom probe that had a specimen manipulator made from a sliding glass seal and a vertical configuration. All subsequent atom probes have vacuum systems fabricated from stainless steel components, and have horizontal configurations.

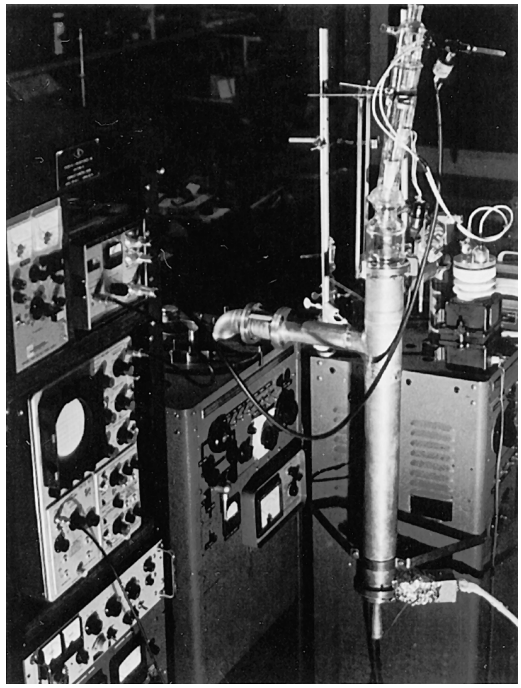

FIG. 2. Photograph of the original atom probe field-ion microscope [9] developed by Panitz, McLane, and Müller in 1968. The field ion microscope section is the glass section (top right) and the single-atom detector is at the bottom of the vertical mass spectrometer. The oscilloscope at the left was used to record the flight times of the ions. (Photograph courtesy J. A. Panitz, S. B. McLane, and E. W. Müller.)

To measure the flight time of the atom, t, a short duration (~10ns) high-voltage pulse is used to remove an ionized atom from the surface of the specimen at a specific time. This pulse is also used to start the timing system. The timing system is stopped when the ion strikes the single atom detector. The mass-to-charge ratio, m/n, of the ion is given by

$$\frac{m}{n} = cV\frac{t^2}{d^2},$$

where c is a constant, d is the flight distance, and V is the total voltage on the specimen. On the original atom probe, the measurement of the flight time was performed on a storage oscilloscope (Fig. 2), whereas in today's instrument it is performed with computer-controlled digital timing systems with a 1-ns time resolution or better. The el-

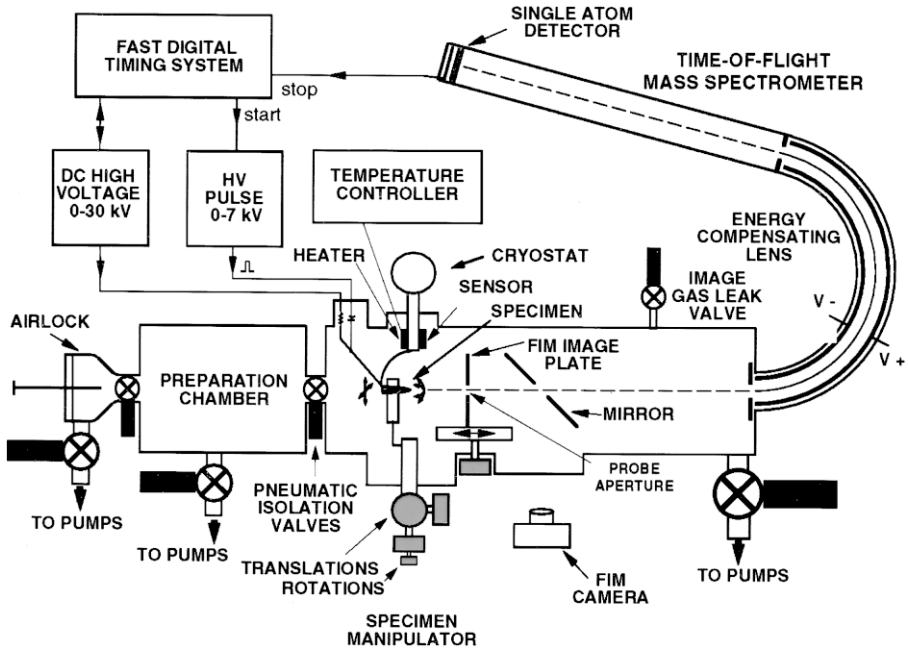

FIG. 3. Schematic diagram of an energy-compensated atom probe that features a 163° Poschenreider lens to improve the mass resolution.

emental identity of the ion is then deduced from its mass-to-charge ratio. This identification process is simpler than in many other types of mass spectrometers because the number of molecular or complex ions is very small, and the number of charge states is usually limited to between one and three different states, and is a characteristic of the element and the temperature of the analysis. Because a time-of-flight mass spectrometer is used, there is no mass restriction, and the atom probe can detect all elements with equal sensitivity.

One of the main limitations of this simple variant was its mass resolving power or mass resolution. Typical values ranged from $m/\Delta m = 100$ to 250, and these low values made it impractical to fully resolve closely spaced isobars in the mass spectrum of complex commercial alloys. This limitation imposed significant restrictions on the quantification of data from some types of alloys in these early instruments. The main source of the limitation is the small energy deficit that is associated with the high-voltage pulse that is used to field evaporate the ions from the specimen. To overcome this limitation, Müller and Krishnaswamy [13] incorporated an energy-compensating lens into the mass spectrometer in 1974. This electrostatic lens was a sector of a torroid, and was based on a design described by Poschenrieder [14]. This lens also has the advantage of filtering out ions with the energy associated with the standing voltage on the specimen, and this dramatically improved the background noise level in the spectra. Later, Mamyrin et al. [15], Kudryatsev et al. [16], and Drachsel et al. [17] all incorporated first-order reflectron lenses into their mass spectrometers for the same purpose. One disadvantage of the reflectron lens is the need for a grounded mesh on the entrance and exit to properly define the field gradient within the lens. This high-transparency (typically >90%) mesh reduces the detection efficiency of ions emitted from the specimen. The typical mass resolution of these energy compensating instruments is $m/\Delta m = 1{,}000$ to 2,500, with some instruments approaching $m/\Delta m = 6{,}000$. At these levels,

the individual isotopes of all the elements are resolvable, and full quantification of the composition is possible for almost all materials. These instruments are referred to as energy-compensated atom probes (ECAP), and a schematic diagram of one is shown in Fig. 3. These commercially available instruments are primarily used for metallurgical applications.

An alternative system may also be used to remove atoms from the surface by replacing the high voltage pulse with a short laser pulse as first described by Kellogg and Tsong in 1980 [18]. This alternative instrument, known as a pulsed laser atom probe (PLAP), is generally applied only to specimens with poor electrical conductivity such as semiconductors and some conducting ceramics.

The atom probe and its variants may be used to identify the elemental species of an individual atom such as an atom segregated to a dislocation, grain boundary, or interphase interface. In these types of experiments the specimen is rotated so that the projected image of that atom in the field ion microscope is aligned with the entrance aperture to the time-of-flight mass spectrometer. This small aperture is generally in the center of the microchannel plate and phosphor screen assembly, on which the field ion image is detected. High-voltage pulses are then applied to the specimen until the atom of interest is field evaporated and analyzed in the mass spectrometer. However, most atom probe analyses involve collecting much larger numbers of atoms. If the analysis is continued by field evaporating atoms without moving the specimen, a cylinder of atoms is collected. If this cylinder was obtained from sampling a single phase, the concentrations of each element present in that phase is obtained by simply counting the number of atoms of each element compared to the total number of atoms. The atom-by-atom data may also be grouped into small blocks of atoms from which the concentrations for each element may be obtained by counting the number of atoms of each element compared to the total number of atoms in the block. In this manner, composition profiles may be obtained across interphase interfaces, grain boundaries, etc. Composition data may also be obtained by collecting this cylinder of atoms across the alternating planes of different composition in ordered alloys to investigate the degree of ordering and the site preference of substitutional elements.

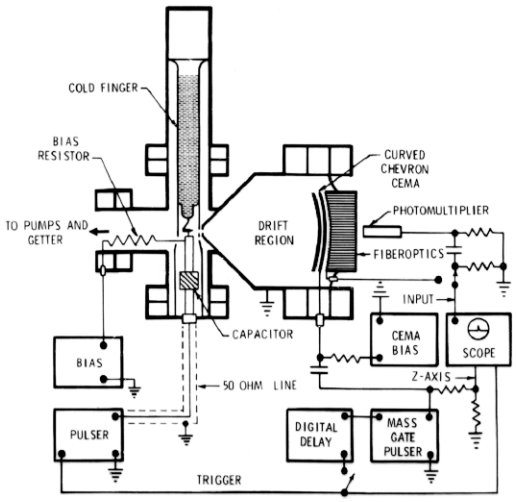

FIG. 4. Schematic diagram of the 10cm or imaging atom probe. This instrument features a detector with a pair of curved microchannel plates and phosphor screen. The detector may be activated for a short time to image a selected elemental species. (Courtesy J. A. Panitz.)

10cm OR IMAGING ATOM PROBE

The next significant step in the development of the atom probe was the introduction of the "10cm atom probe" by Panitz in 1973 [19–21]. In this variant, a relatively large area single atom detector (~75mm in diameter) is positioned 10 to 15cm in front of the specimen, as shown in Fig. 4. The pair of microchannel plates and the phosphor screen of this detector are spherically curved to match the tip-to-screen distance so the flight times of the same mass-to-charge ratio species are identical at all positions on the detector. The phosphor screen is deposited directly onto a conducting layer deposited onto the curved surface of a

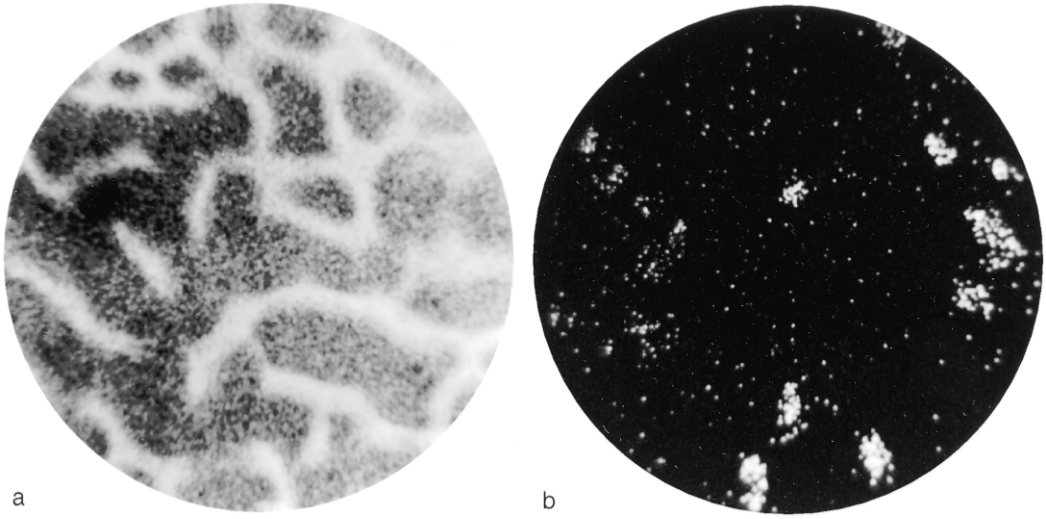

FIG. 5. Field evaporation images obtained from an imaging atom probe. (a) Image formed by the removal of several atomic layers showing the interconnected nature of the chromium-enriched α' phase in Fe-45% Cr, and (b) the cobalt distribution in a Cu-2% Co alloy that contains small cobalt-rich precipitates

fiber optic bundle, with flat surface on the opposite side. This arrangement provides a flat field to record the images on a camera. This assembly is often built into a standard vacuum flange, and can take the place of a viewport. By operating the detector at low gain, a field ion image of the specimen may be obtained. As the tip-to-screen distance is typically two to three times longer than that in a standard field ion microscope, only a portion of the specimen is imaged.

A field desorption, or more correctly a field evaporation image, of the same area may also be obtained by operating the detector at higher gain in the absence of the image gas by either increasing the voltage on the specimen or by applying a high-voltage pulse to field evaporate the specimen. A multilayer field evaporation micrograph of an Fe-45% Cr alloy is shown in Fig. 5(a). The contrast in this image arises from the small local magnification differences between the two phases, which compress or expand the ion trajectories. By connecting the electrical output of the phosphor to a storage oscilloscope, a time spectrum from the area of the specimen defined by the detector can be obtained from a single high-voltage pulse. The amount of each element present may be estimated from the height of the peaks in this spectrum.

The most unique feature of this type of instrument is to image a selected ion species or element by time gating the single atom detector. This selection is performed by only activating the detector for a very short time (typically 10 ns) after the high-voltage field evaporation pulse to coincide when the selected ion species would strike the detector. In this type of image, each dot is the result of an impact of a single ion on the detector. This technique results in an atomic resolution two-dimensional (2D) dot map of the distribution of the selected element in the material, as shown for the Co^{++} species in Fig. 5(b). The cobalt precipitates are clearly evident as the areas of higher dot density. Additional elements may be imaged on successive high voltage pulses by adjusting the time delay. Because of the ability to image a selected element, this type of instrument is now referred to as an imaging atom probe (IAP).

This instrument has been used to perform 3D reconstructions of biological molecules. In this field ion tomography mode, the biological molecule is carefully deposited from an aqueous solution onto the sur-

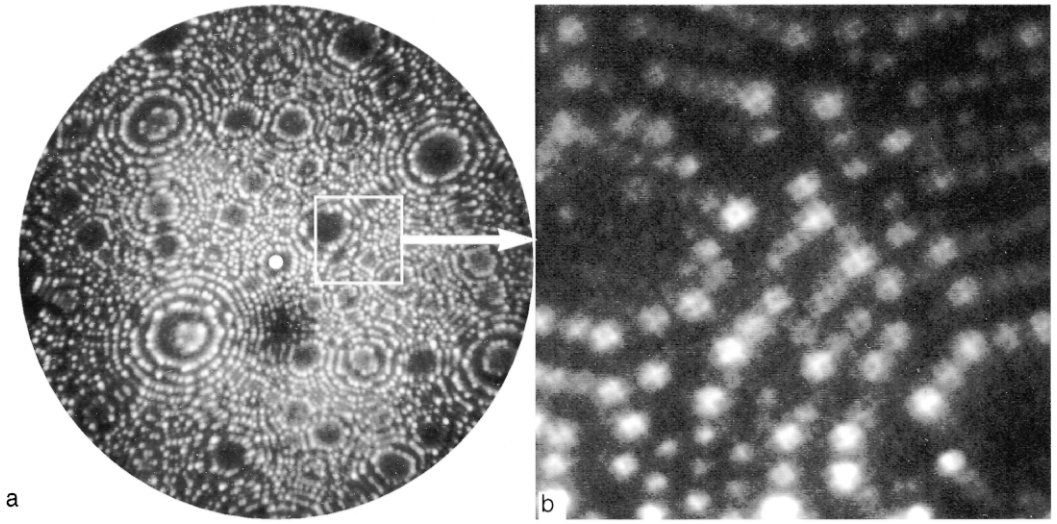

FIG. 6. Comparison of the acceptance angles of a field ion microscope and a 3D atom probe. (a) Field ion image of the Ni_4Mo phase in a model nickel-based superalloy, and (b) a field ion image of the region selected for analysis on the detector of a 3D atom probe. The small white dot in the center of the field ion image in (a) is a simulation of the size of the entrance aperture to the mass spectrometer in a probe aperture type of atom probe.

face of the field ion specimen. The molecule is then encased in an immobile layer of either benzene or water ice that is condensed from the vapor state onto the cryogenic surface. The ice layer is then field desorbed from the surface and its image recorded on the imaging atom probe detector. The region where the biological molecule is present will appear dark (i.e., no signal) in these images. The shape of the biological molecule can then be reconstructed from a series of these images.

The imaging atom probe has only found limited applications in materials science due to the difficulty of quantifying the 2D data from the dot maps. In addition, it is not practical to get correlated maps of all the elements present in the specimen, as material is field evaporated during the recording of each slice so the data for each element are not from the same volume.

THREE-DIMENSIONAL ATOM PROBE (3DAP)

One of the most significant advances in atom probe development was the introduction of a new type of instrument known as a three-dimensional atom probe (3DAP) [22]. Several different variants of this type of instrument have been developed by various atom probe groups, and are described in the following paragraphs. The primary difference between these instruments is the type of position-sensitive single atom-sensitive detector that is used at the end of the mass spectrometer. The basic configuration is the same as the imaging atom probe, with the cryogenically cooled specimen mounted on a goniometer and pointing towards a position-sensitive detector. The use of expensive curved microchannel plates and phosphor screen was no longer necessary, as the difference in the flight distance can be compensated for in the analysis software. This type of 3D atom probe enables the x, y, and z coordinates of each atom in a selected volume in the specimen, together with its mass-to-charge ratio, to be determined. In this paper, the x and y directions are defined to be in the plane of the detector, and the z direction is along the wire axis of the specimen. These data may then be reconstructed in a computer to

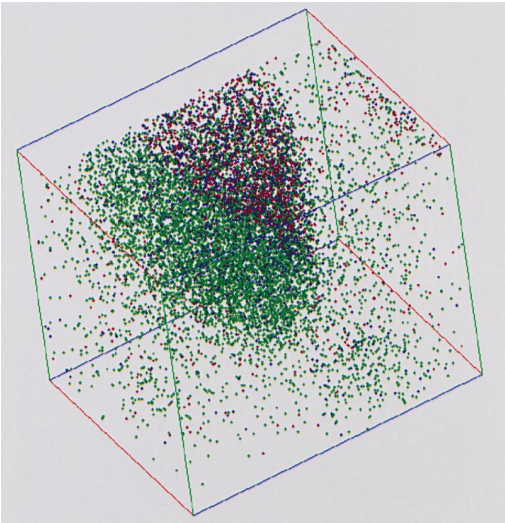

FIG. 7. Atom map of a secondary precipitate in Alloy 718. In this type of representation, a color-coded sphere denotes the position of each atom; Al atoms are red, Ti atoms are blue, and Nb atoms are green. Note the dual γ'-γ'' nature of the precipitate. Box is 11.2 × 12.3 × 14.1nm in extent.

yield the solute distribution in the volume. The acceptance angle of detected ions in these instruments is significantly larger than a classical atom probe, but is still significantly smaller than that available in the field ion image, as shown in Fig. 6. The flight distance is typically 250 to 650mm. A typical sample volume is ~10 × ~10 × ~250nm, and contains approximately 10^6 atoms. The time taken to accumulate this number of atoms is typically 20 h.

Some common examples of the types of analyses that are possible with atom probe tomography [22] are shown in Figs. 7 and 8. The simplest representation is a color-coded dot or a sphere to indicate the position of each type of atom, as shown in Fig. 7 for a secondary precipitate in superalloy Alloy 718. This method is very effective when only the minor elemental species are plotted. This method may be used to visualize precipitation or segregation to features such as interfaces and grain boundaries. Another type of representation is the isoconcentration surface (often shortened to the isosurface) which is the 3D equivalent to a contour plot. To calculate this surface, the ion-by-ion data are divided into small volume elements (or voxels) and the concentrations of the element of interest are calculated. The mean surface through a specific concentration over the entire data set is then plotted in three dimensions, as shown in Fig. 8 for the network structure of the chromium-enriched α' phase in an Fe-32% Cr alloy aged for 10,000 h at 470°C. This representation enables the morphology of features such as precipitates to be visualized.

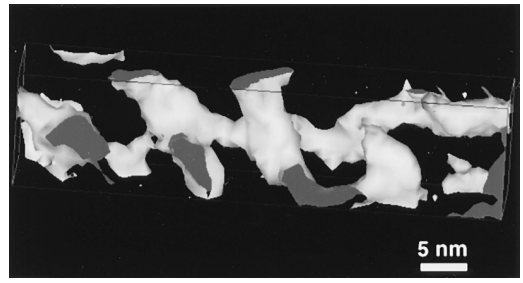

FIG. 8. Isoconcentration surface of the chromium-enriched α' phase in Fe-32% Cr aged 10,000 h at 470°C.

One key component of all the 3D atom probes is the high-speed graphics-oriented computers that are required to analyze the data. One of the main advantages of atom probe tomography, apart from the larger number of atoms collected, is that the features present in the 3D data may be analyzed in a computer after the experiment is completed. For example, composition profiles may be obtained that are normal to the interfaces of precipitates or grain boundaries. In contrast, in the classical atom probe (and in the 3D atom probe), the analysis direction is always to a first approximation along the specimen axis.

Precursory Developments

The first prototype of a 3D atom probe was implemented in early 1986 by Miller, based on plans initiated in 1984. A previously unpublished sketch of this early prototype is shown in Fig. 9. This instrument was based on the imaging atom probe configuration with two secondary detectors. Both second-

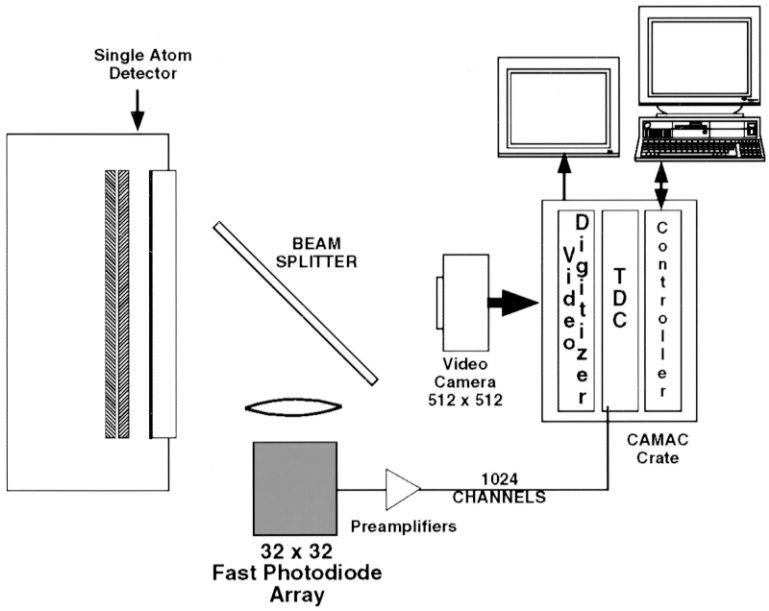

FIG. 9. A sketch of the prototype 3D atom probe proposed by Miller. The dual external detectors consist of a CCD camera and a 32 × 32 array of photodiodes.

ary detectors were external to the vacuum system, and are focused on the light output from the imaging atom probe detector with a beam splitter and lenses. The first detector was a CCD camera that was used to determine the x and y position of the ions striking the detector. The use of video recording of the images from the imaging atom probe was pioneered by Panitz [23]. The second detector was a 32 × 32 array of photodiodes to determine the flight times with the use of 1,024 channels of time-to-digital converters. Each photodiode was designed to map to a 4 × 4 subset of pixels on the CCD camera. However, initial experiments with this type of triggerable CCD camera indicated that its gain was very marginal at this time, and resulted in having to operate the imaging atom probe detector at extremely high gain. In addition, this version also suffered from excessive background noise on the camera detector. This approach was to reemerge a few years later as the optical atom probe.

Concurrently in 1985, Schiller et al. [24] implemented a computerized imaging system for field ion microscopy and time gated time-of-flight imaging. The detector was based on a pair of microchannel plates and a resistive anode. The x and y coordinates of each image gas ion striking the detector were determined from the relative electrical charges measured at the four corners of the resistive anode. No attempts were made to use this instrument as an atom probe.

Position-Sensitive Atom Probe (PoSAP)

The first commercial 3D atom probe was the position-sensitive atom probe that was developed by Cerezo et al. in 1988 [25, 26]. The instrument featured the same basic configuration of an imaging atom probe with the important distinction that the single-atom detector was able to encode the positions of the impacts of each ion, as shown in Fig. 10. The single-atom detector featured a wedge-and-strip anode developed by Martin et al. [27] in 1981, in place of the phosphor screen, as shown in Fig. 10. The position of the impact of the ion on the single-atom detectors is determined from the relative amounts of electrical charge

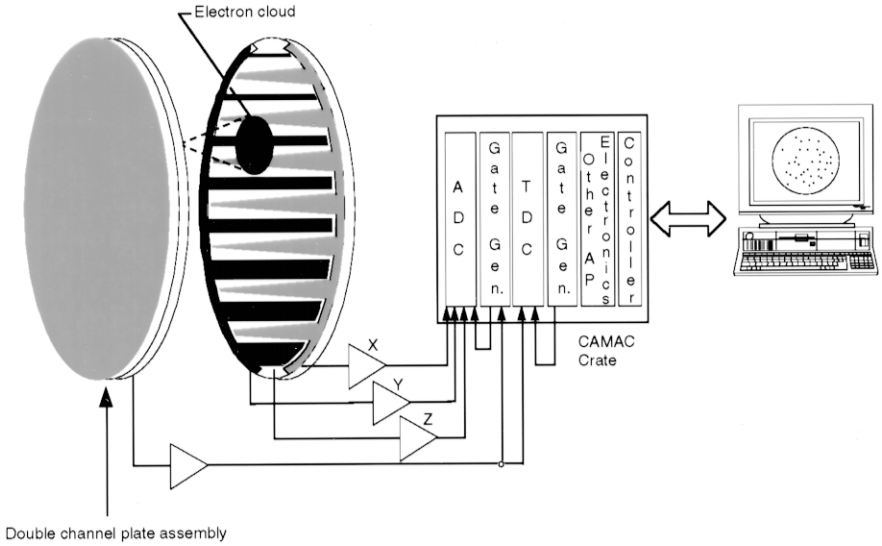

FIG. 10. Schematic diagram of the position-sensitive atom probe that was developed by Cerezo et al. This instrument features a wedge-and-strip detector to determine the positions of impact of the ions on the detector from the relative charge on the three anodes. Note the electron cloud from the microchannel plate typically covers several of the wedges and strips.

measured on the three electrodes of the wedge-and-strip detector. Because taking the timing signals to determine the flight times of the ion from the anodes would interfere with the charge measurements, these signals are taken from the rear face of the microchannel plates. One of the main limitations of this variant was that its detection efficiency was rather low. This was mainly due to the problem of multiple ions striking the detector on the same field evaporation pulse because the wedge-and-strip anode could only determine the average position of the multiple impacts, and so these ions were lost from the analysis.

As a refinement of this instrument to minimize this multihit problem and to permit higher data collection rates, Kelly et al. [28] proposed different configurations of the wedge-and-strip anode with additional electrodes and segmentation of the detector into different subdetectors.

Tomographic Atom Probe (TAP)

A different approach was adopted by Bostel et al. [29, 30] in 1989, in the tomographic atom probe. A schematic diagram of this instrument is shown in Fig. 11. In this design, the phosphor screen was replaced by a 10 × 10 array of anodes deposited directly onto a viewport with an electrical feedthrough for each anode, as shown in Fig. 12. The electron cloud that is produced by the Z-stack of three microchannel plates spreads out in the small gap between the microchannel plate and the anodes so that it covers several anodes. The position of the ion's impact could be determined from the relative charge on each anode. The stop signal for the time-of-flight is taken from the rear of this stack of microchannel plates. This signal is used to trigger one of up to eight banks of charge-to-digital converters. This method has the advantage of not being limited, in most cases, by multiple ions striking the detector on a field evaporation pulse. This instrument also incorporated a negatively-biased high transparency mesh in front of the microchannel plate to improve the detection efficiency of these types of detectors by returning the secondary electrons produced when a primary ion hit the microchannel plate between the chan-

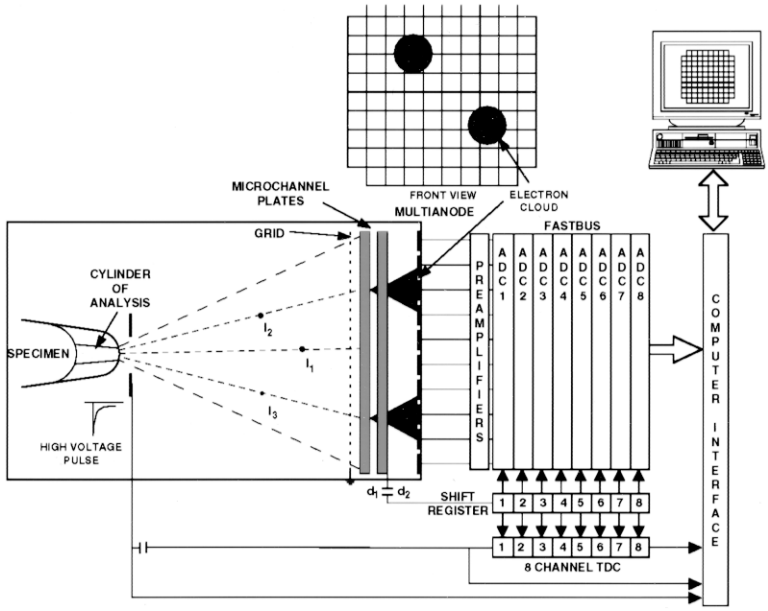

FIG. 11. Schematic diagram of the tomographic atom probe developed by Bostel et al. This instrument features a 10×10 array of anodes and a z-stack of three microchannel plates. Note the electron cloud from the rear of the third microchannel plate spreads out to cover several anodes. The position of the ion is calculated from the amounts of charge on the anodes.

nels. This instrument also featured a negative field evaporation pulse on the counter electrode in front of the specimen instead of the traditional capacitively-coupled positive high-voltage pulse applied to the specimen. This configuration permits a matched impedance line to be maintained, and slightly improves the mass resolution in instruments without energy compensation.

Optical Atom Probe (OAP) and Its Derivatives

In 1991, the optical atom probe reemerged with a higher resolution CCD camera and an external image intensifier between the primary detector and the CCD camera [31, 32]. A schematic diagram of this instrument is shown in Fig. 13. The external image intensifier also solved random noise problems because it could be used to selectively operate the detector only when genuine ions would be collected in the mass spectrometer. The use of an external image intensifier was developed by Kellogg, in 1987, for time gating an imaging atom probe [33]. One of the design features of the optical atom probe was the ability to convert existing imaging atom probes into 3D atom probes by the simple addition of external components. By operating the detector at low gain, a field ion image of the exact analysis region may be viewed in real time on the single atom detector. Although field ion images may be recorded on the detectors of the position-sensitive atom probe and the tomographic probe, the imaging process requires some time to accumulate the information. The optical atom probe also suffered from the loss of data from multiple ions striking the detector on the same field evaporation pulse. This variant is now the basis of several different implementations.

In 1994, Cerezo et al. [34] developed an external dual detection system to minimize the multihit problem. This instrument, known as the optical position-sensitive atom probe, included both an image intensified CCD camera to determine the impact

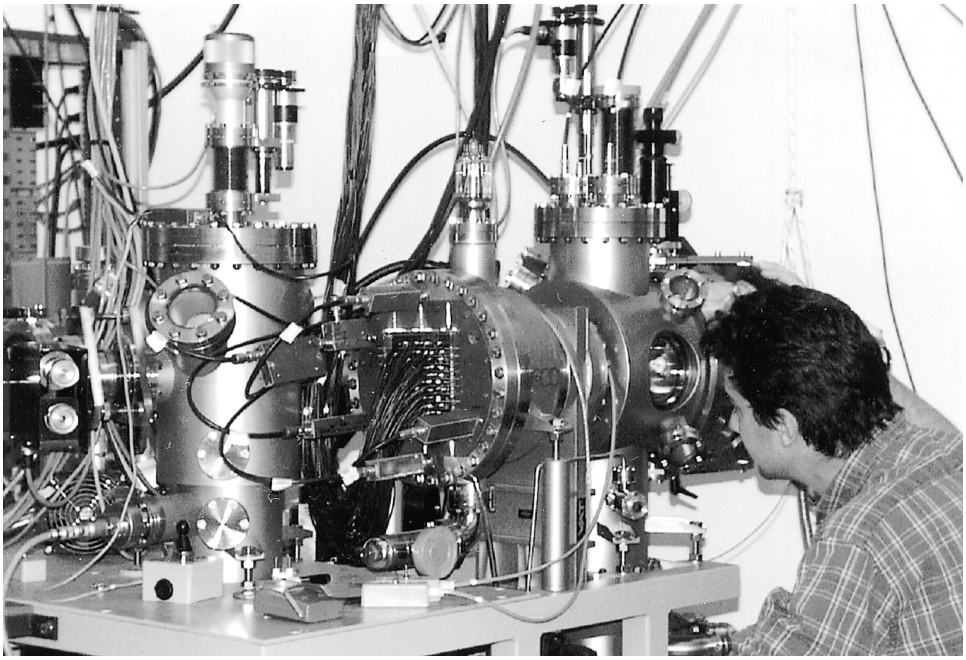

FIG. 12. Photograph of the tomographic atom probe. (Courtesy D. Blavette and B. Deconihout.) The 10 × 10 array of anodes is evident at the end of the mass spectrometer.

positions and a second image intensifier with an 8 × 10 multianode detector, as shown in Fig. 14. Each anode was connected to an additional set of preamplifiers and time-to-digital converters. This configuration enables the time-of-flight information from the primary detector to be linked to the time-of-flight information from the anodes so that area covered by one of the anodes could be assigned to one of the positions of the primary impact determined by the CCD camera. In this method, two or more ions with the same mass-to-charge ratio striking the primary detector at the same time could be distinguished if they did not strike the same anode, and therefore, be properly assigned. Up to this point, all three-dimensional atom probes used linear time-of-flight mass spectrometers, and therefore, suffered from relatively low mass resolution. In 1996, Sijbrandij et al. [35] incorporated a reflectron lens to increase the mass resolution to $\sim m/\Delta m = 500$.

Recently, Deconihout et al. [36] introduced another variant that uses a CCD camera for positioning the ions. A schematic diagram of this instrument, which was called an optical tomographic atom probe (OTAP), is shown in Fig. 15. In this instrument, the phosphor screen on the primary detector was divided into transparent strip anodes each connected to a preamplifier and a time-to-digital converter for the time-of-flight information. This arrangement essentially combined the dual detector configuration into a single detector. To achieve the same function, Miller [37] also proposed a modification of the external image intensifier of the optical atom probe to incorporate a 16 × 2 array of transparent anodes in place of the normal phosphor screen.

SPECIMEN PREPARATION

In addition to the developments in atom probe instrumentation, major improvements have been accomplished in specimen preparation techniques. The requirements

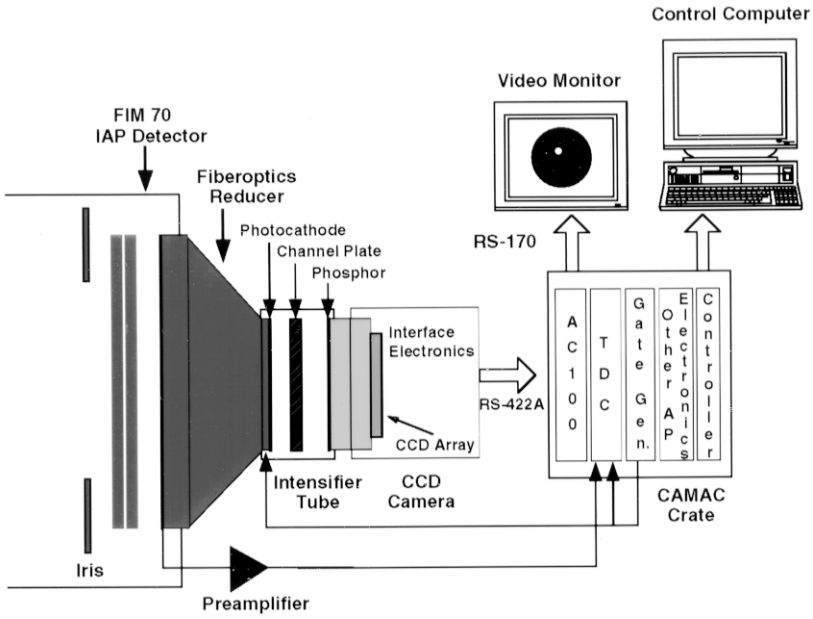

FIG. 13. Schematic diagram of the optical atom probe developed by Miller. This instrument features an external gated image intensifier and a CCD camera.

of a field ion specimen are a sharp needle with a cylindrical cross section, an end radius of less than ~50nm, a taper angle of <10°, and some electrical conduction. The cylindrical symmetry is especially important in the 3D atom probe, as the magnification and thus the lateral x and y distances are dependent on the local radius.

Standard recipes have been developed that enable almost all metallic systems to be electropolished or chemically etched [1, 2]. The starting material is usually a square bar (typically 0.5 × 0.5 × 10mm) cut from the bulk material or a wire. In some cases where chemical etching or electropolishing are not possible, ion-milling techniques may

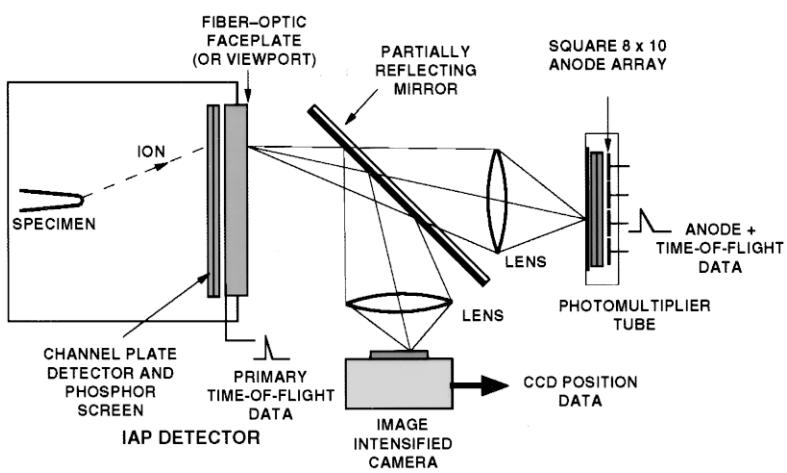

FIG. 14. Schematic diagram of the optical position-sensitive atom probe developed by Cerezo et al. This instrument features a pair of secondary detectors to decode the position and flight time of each ion: a CCD camera and an 8 × 10 array of anodes.

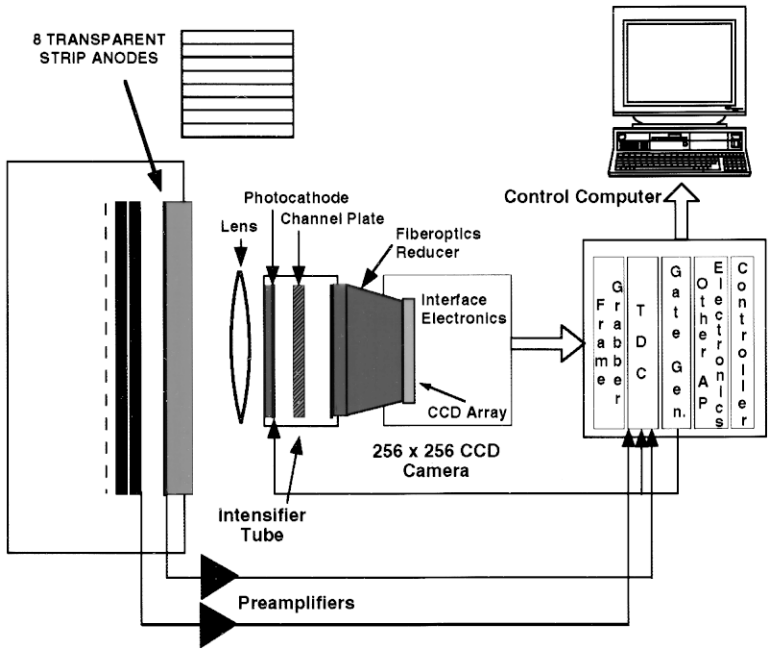

FIG. 15. Schematic diagram of the optical tomographic atom probe developed by Deconihout et al. This instrument features a CCD camera to determine the positions, and the phosphor screen is divided into transparent strip anodes to determine the flight times.

be used. Specimens can usually be resharpened after an atom probe experiment with the use of micropolishing or pulse polishing [1, 2]. Recently, techniques based on ion milling with a focussed ion beam have enabled atom probe needle-shaped specimens to be fabricated from thin films [38].

Because the analyzable volume is extremely small in a typical atom probe specimen, methods based on preselection in the transmission electron microscope and pulse polishing [1, 39] or ion milling [40] have been developed to remove extraneous material. These methods enable a feature of interest, such as a grain boundary or precipitate, to be positioned in the analyzable region of the specimen. In addition, examination of the field ion specimen in the electron microscope can provide additional information such as the orientation of the grains and the crystal structure of precipitates. Examination of the specimen in the transmission electron microscope at the end of a 3D atom-probe experiment is performed to measure the end radius of the needle at a known applied voltage to obtain a precise calibration of the magnification.

FUTURE DIRECTIONS

There is little doubt that the development of the atom probe will continue. One possible avenue is to develop new types of single atom sensitive detectors. Some possibilities are a detector based on delay lines [41] or totally integrated solid-state detectors based on arrays of photodiodes or other types of sensors. There is also scope to improve both the mass resolution and detection efficiency with better methods of energy compensation at large acceptance angles and with higher transmission efficiency. Incremental improvements in performance will be gained with better solid-state high-voltage pulsers capable of operating at higher frequencies and voltages. It should be possible to increase these rates by up to a factor of ten, with a marked decrease in the time

required for an analysis. Another area that has been investigated recently is to operate an atom probe remotely over the Internet [42]. This mode of operation would make the instrument available to a significantly larger number of scientists. The methods of analyzing the 3D data are still in their early stages of development, so significant improvements are probable.

In attempts to extend the capability of the atom probe to other specimen geometries and materials, several groups are developing a new type of atom probe originally proposed by Nishikawa et al. [43], and known as a scanning atom probe or a local electrode atom probe [44, 45]. This type of instrument features a local counter electrode, which can be moved laterally over the surface of a flat specimen that contains a number of natural or fabricated protrusions. One of these protrusions or emitters is then selected for analysis by accurately aligning the local electrode above and very close to the apex of the emitter. This type of instrument should offer high rates of data collection, as the voltage pulse required to field evaporate ions from the specimen is much lower in amplitude and can, therefore, be generated at significantly higher frequencies than normal high voltage pulses. It is possible that these local electrodes may be used to advantage on normal atom probes so that some of these potential benefits may be realized.

The author would like to thank Dr. D. J. Larson and K. F. Russell for their assistance. This research was sponsored by the Division of Materials Sciences, U.S. Department of Energy, under contract DE-AC05-96OR22464 with Lockheed Martin Energy Research Corp., and through the SHaRE Program under contract DE-AC05-76OR00033 with Oak Ridge Associated Universities. This research was conducted utilizing the Shared Research Equipment User Program facilities at ORNL. The submitted manuscript has been authored by a contractor of the U.S. Government under contract No. DE-AC05-96OR22464. Accordingly, the U.S. Government retains a nonexclusive, royalty-free license to publish or reproduce the published form of this contribution, or allow others to do so, for U.S. Government purposes.

References

1. M. K. Miller and G. D. W. Smith: *Atom Probe Microanalysis: Principles and Applications to Material Problems*, Materials Research Society, Pittsburgh (1989).
2. M. K. Miller, A. Cerezo, M. G. Hetherington, and G. D. W. Smith: *Atom Probe Field Ion Microscopy*, Oxford University Press, Oxford, UK, (1996).
3. M. K. Miller: *Atom Probe Tomography: Analysis at the Atomic Level*, Plenum, New York (1999).
4. G. L. Kellogg: Field ion microscope studies of single-atom diffusion and cluster nucleation on metal surfaces. *Surface Sci. Rep.* 21:1–88 (1994).
5. T. T. Tsong: *Atom Probe Field Ion Microscopy*, Cambridge University Press, UK, (1990).
6. E. W. Müller: The field ion microscope. *Z Physik.* 131:136–142 (1951)
7. E. W. Müller: Electron microscopic investigation of field cathodes. *Z. Physik.* 106:541–550 (1937).
8. E. W. Müller, J. A. Panitz, and S. B. McLane: The atom-probe field ion microscope. *Rev. Sci. Instrum.* 39:83–86 (1968).
9. J. A. Panitz: The Atom Probe FIM. Ph.D. Thesis. The Pennsylvania State University (1969).
10. E. W. Müller: Field-ionization and field-ion microscopy. *Adv. Electron. Electron Phys.* 13:83–179 (1960).
11. R. Vanselow and W. A. Schmidt: Field evaporation of platinum at high temperatures in UHV and the presence of oxygen: Mass spectrometric analysis of surface species. *Z. Naturforsch* A21:1690–1696 (1966).
12. D. F. Barofsky and E. W. Müller: Mass spectrometric analysis of low-temperature field evaporation. *Surface Sci.* 10:177–196 (1968).
13. E. W. Müller and S. V. Krishnaswamy: Energy deficits in pulsed field evaporation and deficit compensated atom-probe designs. *Rev. Sci. Instrum.* 45:1053–1059 (1974).
14. W. P. Poschenrieder: Multiple-focusing time-of-flight mass spectrometers: Part II TOFMS with equal energy acceleration. *Int. J. Mass Spectrom. Ion Phys.* 9:357–373. (1972).
15. B. A Mamyrin, V. I. Karataev, D. V. Shmikk, and V. A. Zagulin: The mass-reflectron, a new nonmagnetic time-of-flight mass spectrometer with high resolution. *Soviet Phys. JEPT* 37:45–48 (1973).
16. A. N. Kudryavtsev, N. V Nikonenko, B. M. Dubenskii, and D. V. Shmikk: Atom probe with compensation for the scatter in the ion kinetic energies. *Sov. Tech. Phys. Lett.* 15:261–264 (1989).
17. W. Drachsel, L. v. Alvensleben and A. J. Melmed:

Time focusing in a field pulsed atom-probe with a reflectron. *J. Phys.* 50-C8:541–545 (1989).

18. G. L. Kellogg and T. T. Tsong: Pulsed-laser atom-probe field-ion microscopy. *J. Appl. Phys.* 51:1184–1193 (1980).
19. J. A. Panitz: The 10 cm atom probe. *Rev. Sci. Intrum.* 44:1034–1038 (1968).
20. J. A. Panitz: Field desorption spectrometer. U.S. Patent No. 3,868,507 (1975).
21. J. A. Panitz: Imaging atom-probe mass spectroscopy. *Prog. Surface Sci.* 8:219–262 (1978).
22. M. K. Miller: Three-dimensional atom probes. *J. Microsc.* 186:1–16 (1997).
23. J. A. Panitz: Video recording of low intensity CEMA images. *J. Vac. Sci. Technol.* 17:757–758 (1980).
24. T. Schiller, U. Weigmann, S. Jaenicke, and J. H. Block: Computerized imaging system for field ion microscopy. *J. Phys.* 47-C2:479–484 (1986).
25. A. Cerezo, T. J. Godfrey, and G. D. W. Smith: Development and initial applications of a position-sensitive atom probe. *J. Phys.* 49-C6:25–30 (1988).
26. A. Cerezo, T. J. Godfrey, and G. D. W. Smith: Application of a position-sensitive detector to atom probe microanalysis. *Rev. Sci. Instrum.* 59:862–866 (1988).
27. C. Martin, P. Jelinsky, M. Lampton, R. F. Malina, and H. O. Anger: Wedge-and-strip anodes for centroid-finding position-sensitive photon and particle detectors. *Rev. Sci. Instrum.* 52:1067–1074 (1981).
28. L. M. Holzman, T. F. Kelly, and P. P. Camus: Position-sensitive detector providing position information with enhanced reliability and performance. U.S. Patent No. 5,347,132 (1994).
29. A. Bostel, D. Blavette, A. Menand, and J. M. Sarrau: Toward a tomographic atom probe. *J. Phys.* 50-C8:501–506 (1989).
30. B. Deconihout, A. Bostel, A. Menand, J. M. Sarrau, M. Bouet, S. Chambreland, and D. Blavette: On the development of a 3D tomographic atom probe. *Appl. Surface Sci.* 67:444–450 (1993).
31. M. K. Miller: Concepts in atom probe designs. *Surface Sci.* 246:428–433 (1991).
32. M. K. Miller: Implementation of the optical atom probe. *Surface Sci.* 266:494–500 (1992).
33. G. L. Kellogg: Ion signal calibration in the imaging atom-probe with an external time-gated image intensifier. *Rev. Sci. Instrum.* 58:38–42 (1987).
34. A. Cerezo, T. J. Godfrey, J. M. Hyde, S. J. Sijbrandij, and G. D. W. Smith: Improvements in three-dimensional atom probe designs. *Appl. Surface Sci.* 76/77:374–381 (1994).
35. S. J. Sijbrandij, A. Cerezo, T. J. Godfrey, and G. D. W. Smith: Improvements in the mass resolution of the three-dimensional atom probe. *Appl. Surface Sci.* 94/95:428–433 (1996).
36. B. Deconihout, L. Renaud, G. Da Costa, M. Bouet, A. Bostel, and D. Blavette: Implementation of an optical TAP: Preliminary results. *Ultramicroscopy* 73:253–260 (1998).
37. M. K. Miller: A transparent anode array detector for 3D atom probes. *Microsc. Microanal.* 4(Suppl. 2):80–81 (1998).
38. D. J. Larson, D. T. Foord, A. K. Petford-Long, T. C. Anthony, I. M. Rozdilsky, A. Cerezo, and G. D. W. Smith: Focused ion beam milling for atom probe field ion microscopy specimen preparation: Preliminary experiments. *Ultramicroscopy* 75:147–159 (1998).
39. A. Henjered and H. Norden: A controlled specimen preparation technique for interface studies with atom probe field-ion microscopy. *J. Phys. E. Sci. Instrum.* 16:617–619 (1983).
40. K. B. Alexander, P. Angelini, and M. K. Miller: Precision ion milling of field-ion specimens. *J. Phys.* 50-C8:549–554 (1989).
41. M. R. Williams and S. E. Sobottka: High resolution two dimensional readout of microchannel plates with large area delay lines. *IEEE Trans. Nucl. Sci.* 36:227–229 (1989).
42. M. K. Miller and D. J. Larson: Remote atom probe field ion microscopy. *Ultramicroscopy* 79:259–264 (1999).
43. O. Nishikawa and M. Kimoto: Toward a scanning atom probe. *Appl. Surface Sci.* 76/77:424–430 (1994).
44. T. F. Kelly, P. P. Camus, D. J. Larson, L. M. Holzman, and S. S. Bajikar: On the many advantages of local electrode atom probes. *Ultramicroscopy* 62:29–42 (1996).
45. P. P. Camus, D. J. Larson, L. M. Holzman, and T. F. Kelly: A new electronic detector of FIM and AP: Initial WoW results. *J. Phys. IV* (Suppl. to *J. Phys. III*, 6): C5:291–295 (1996).

Received December 1998; accepted January 1999.